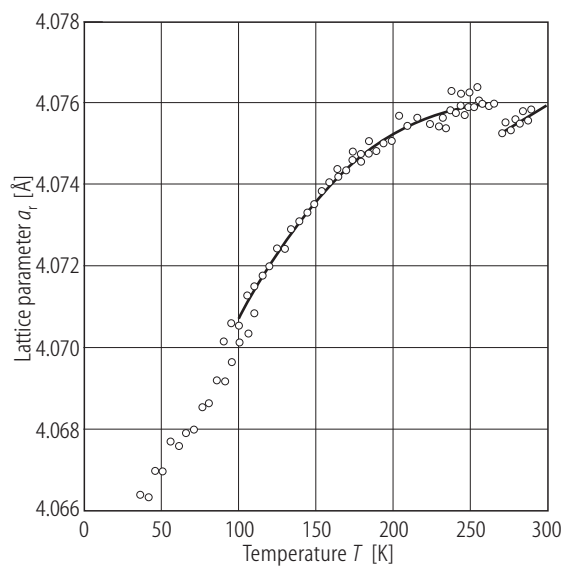


**No. 1B-c19  $\text{Pb}(\text{Sc}_{1/2}\text{Ta}_{1/2})\text{O}_3$**   
 $(M = 368.2)$

1a	Ferroelectricity in $\text{Pb}(\text{Sc}_{1/2}\text{Ta}_{1/2})\text{O}_3$ was discussed by Smolenskii et al. in 1959.		59Smo
b	phase	II	I
	state	F	P
	crystal system	rhombohedral <sup>a)</sup>	cubic
	space group	$\text{R}\bar{3}\text{m} - \text{C}_{3v}^5$ or $\text{R}\bar{3} - \text{C}_3^4$	$\text{Pm}\bar{3}\text{m} - \text{O}_h^1$
	$\Theta$ [K]	270.0(1)	
2a	Crystal growth: flux method.		80Set1
3a	$a = b = c = 4.0760(2)$ Å at RT.		85Gro
b	Crystal structure: The large number of superstructure lines and great intensity in $\text{Pb}(\text{Sc}_{1/2}\text{Ta}_{1/2})\text{O}_3$ indicates that the degree of ordering of $\text{Sc}^{3+}$ and $\text{Ta}^{5+}$ ions is greater than in $\text{Pb}(\text{Sc}_{1/2}\text{Nb}_{1/2})\text{O}_3$ .		59Ism
4	Lattice distortion: Fig. 1B-c19-001.		
5a	Dielectric constant: Figs. 1B-c19-002...1B-c19-008.		
c	Polarization: Fig. 1B-c19-009. Coercive field: Fig. 1B-c19-010.		
7b	Electrostriction: Table 1B-c19-001.		
9a	Birefringence: Fig. 1B-c19-011.		
14	Electron microscopic observations of ordered and disordered phases of $\text{Pb}(\text{Sc}_{1/2}\text{Ta}_{1/2})\text{O}_3$ : see		86Ran
	Observations by electron diffraction of new super-lattice reflections and diffuse scattering in both the paraelectric and ferroelectric phases: see		86Ran
15a	Domain structure was observed at low temperature by polarized light <sup>a)</sup> and transmission electron microscope <sup>b)</sup> . High resolution electron microscopic study of domain structure:		<sup>a)</sup> 81Set <sup>b)</sup> 86Ran 92Pen, 93Pen
16	$\text{Pb}(\text{Sc}_{1/2}\text{Ta}_{1/2})\text{O}_3$ thin film: see		91Pat

**Table 1B-c19-001.**  $\text{Pb}(\text{Sc}_{1/2}\text{Ta}_{1/2})\text{O}_3$  (crystal).  $C$ ,  $Q_h$ ,  $\Delta T/\Delta p$  for various samples [80Set2].  $C$ : Curie-Weiss constant.  $Q_h$ : electrostrictive constant,  $Q_h = Q_{11} + 2Q_{12}$ .  $s$ : order parameter.  $\delta$ : diffuseness parameter calculated from the formula  $\kappa^{-1} = 1/\kappa_{\max} + (2Q_h C)^2 (p - p_0(T))^2 / 2\kappa_{\max} \delta^2$ , where  $p_0(T) = (Q_{\max} - T)/2Q_h C$ , and  $\kappa_{\max}$  is the maximum value of  $\kappa$  at  $p = 0$  and  $Q_{\max}$  is the temperature where  $\kappa = \kappa_{\max}$ .

	Diffuseness parameters	$C$ [ $\cdot 10^5 \text{ K}$ ]	$Q_h$ [ $\cdot 10^{-2} \text{ m}^4 \text{ C}^{-2}$ ]	$\Delta T/\Delta p$ [ $\cdot 10^{-8} \text{ KPa}^{-1}$ ]
disordered crystal ( $s = 0.35$ )	$\delta = 45^\circ$ ( $52^\circ$ ) $1/\kappa_{\max} = 8.6 \cdot 10^{-5}$	2.8	0.88	−3.6
disordered ceramic ( $s = 0.40$ )	$\delta = 38^\circ$ ( $45^\circ$ ) $1/\kappa_{\max} = 5.0 \cdot 10^{-5}$	3.0	0.95	−3.8
ordered ceramic ( $s = 0.85$ )		2.9	0.80(5)	−3.1
ordered crystal ( $s = 0.80$ )		2.4	0.85	−2.0
average value		2.80(25)	0.87(6)	



**Fig. 1B-c19-001.**  $\text{Pb}(\text{Sc}_{1/2}\text{Ta}_{1/2})\text{O}_3$  (crystal).  $a_r$  vs.  $T$  [85Gro].  $a_r$ : unit cell parameter for the rhombohedral axis.

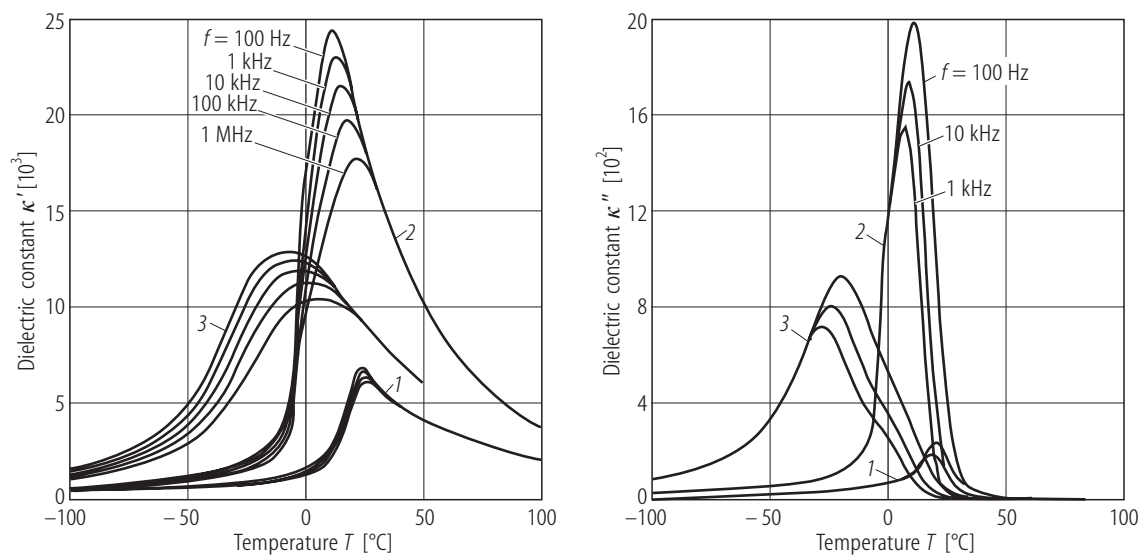


**Fig. 1B-c19-002.**  $\text{Pb}(\text{Sc}_{1/2}\text{Ta}_{1/2})\text{O}_3$  (ceramics).  $\kappa'$ ,  $\kappa''$  vs.  $T$  [93Chu]. Parameter:  $f$ . Curve 1: stoichiometric highly ordered sample ( $s = 0.90$ ). 2: stoichiometric highly disordered sample ( $s = 0$ ). 3: highly disordered sample ( $s = 0$ ) with lead vacancies.  $s$ : order parameter.

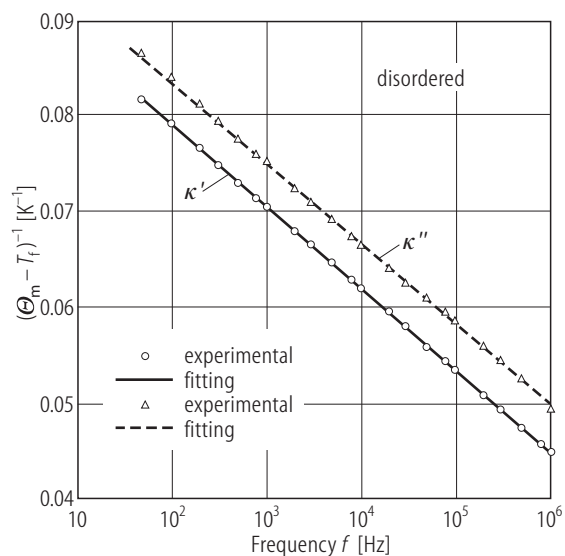


**Fig. 1B-c19-003.**  $\text{Pb}(\text{Sc}_{1/2}\text{Ta}_{1/2})\text{O}_3$  (ceramics).  $(\Theta_m - T_f)^{-1}$  vs.  $T$  [93Chu].  $\Theta_m$ : the temperatures of  $\kappa'$  or  $\kappa''$  maximum.  $T_f$ : a constant in the Vogel-Fulcher equation  $f = f_0 \exp[-E/(\Theta_m - T_f)]$ . The solid and broken curves are fitting of the Vogel-Fulcher equation with  $f_0 = 1.65 \cdot 10^{11}$  Hz,  $T_f = 270.78$  K,  $E = 267.8$  K, and  $f_0 = 9.99 \cdot 10^{11}$  Hz,  $T_f = 265.8$  K,  $E = 275.9$  K, respectively. Stoichiometric highly disordered sample.

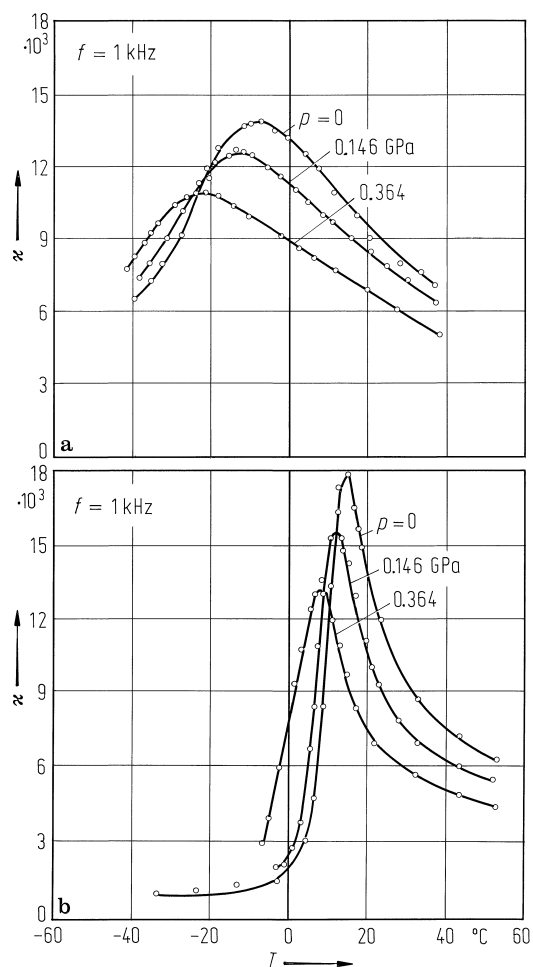


**Fig. 1B-c19-004.**  $\text{Pb}(\text{Sc}_{1/2}\text{Ta}_{1/2})\text{O}_3$  (crystal).  $\kappa$  vs.  $T$  [80Set2]. Parameter:  $p$ . **(a)**  $s = 0.35$  (disordered). **(b)**  $s = 0.80$  (ordered).  $s$ : order parameter.

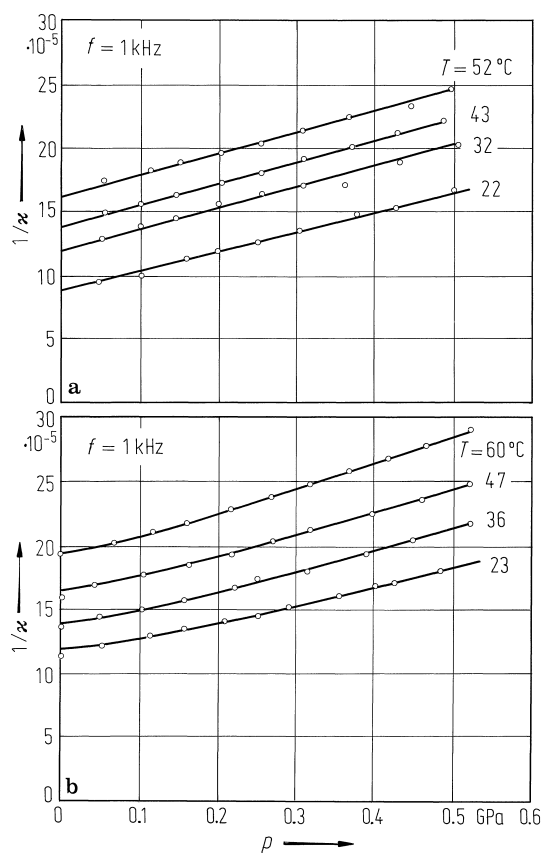


**Fig. 1B-c19-005.**  $\text{Pb}(\text{Sc}_{1/2}\text{Ta}_{1/2})\text{O}_3$  (crystal).  $\kappa^{-1}$  vs.  $p$  [80Set2]. Parameter:  $T$ . **(a)**  $s = 0.80$  (ordered). **(b)**  $s = 0.35$  (disordered).  $s$ : order parameter.

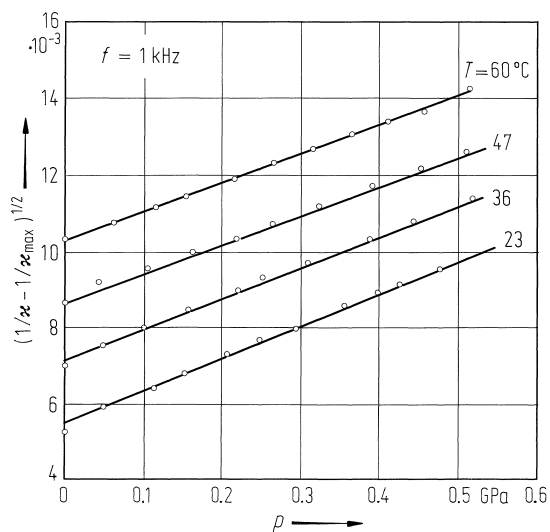


**Fig. 1B-c19-006.**  $\text{Pb}(\text{Sc}_{1/2}\text{Ta}_{1/2})\text{O}_3$  (crystal).  $(\kappa^{-1} - \kappa_{\max}^{-1})^{1/2}$  vs.  $p$  [80Set2]. Parameter:  $T$ .  $\kappa_{\max}$ : the maximum value of  $\kappa$  at  $p = 0$ . Specimen: disordered single crystals.



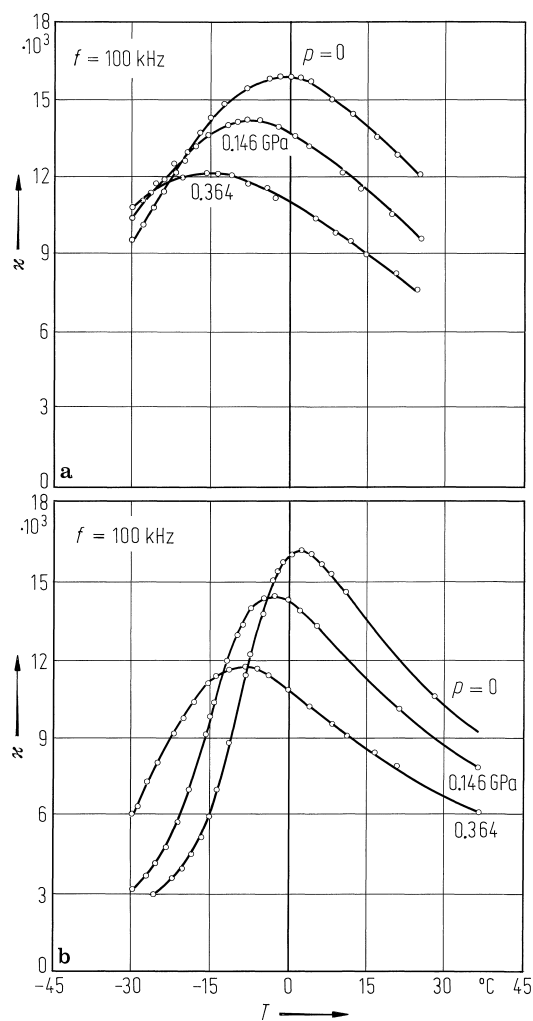


**Fig. 1B-c19-007.**  $\text{Pb}(\text{Sc}_{1/2}\text{Ta}_{1/2})\text{O}_3$  (crystal).  $\kappa$  vs.  $T$  [80Set2]. Parameter:  $p$ . (a)  $s = 0.40$  (disordered). (b)  $s = 0.85$  (ordered).  $s$ : order parameter.

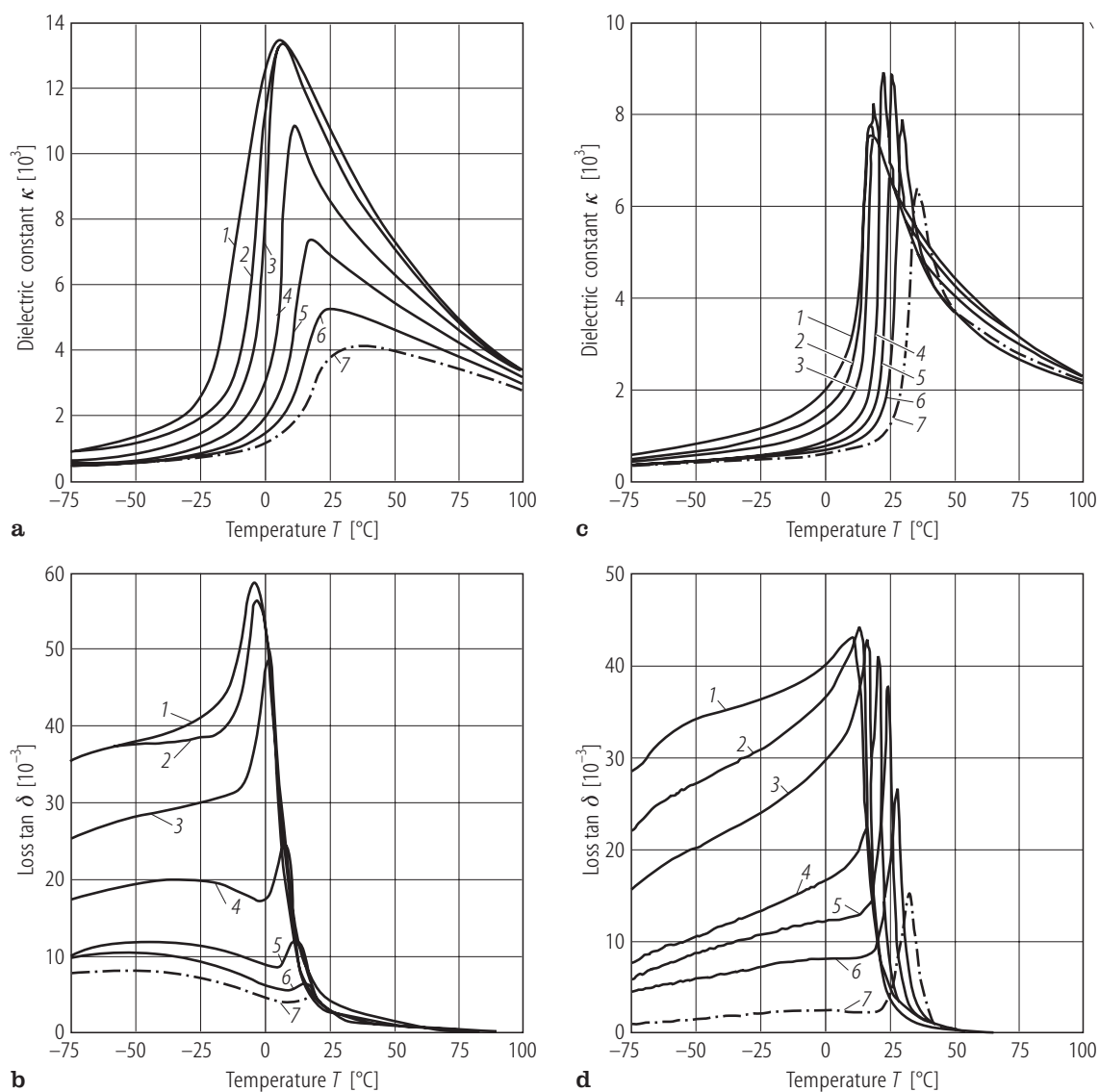


**Fig. 1B-c19-008.**  $\text{Pb}(\text{Sc}_{1/2}\text{Ta}_{1/2})\text{O}_3$  (ceramics).  $\kappa'$ ,  $\tan \delta$  vs.  $T$  [92Dag]. Parameter:  $E_{\text{bias}}$ . (a), (b): disordered sample ( $s = 0$ ). (c), (d): ordered sample ( $s = 0.84$ ).  $s$ : degree of order determined by X-ray diffraction. Curve 1:  $E_{\text{bias}} = 0$ ; 2:  $0.25 \text{ MVm}^{-1}$ ; 3:  $0.5 \text{ MVm}^{-1}$ ; 4:  $1.0 \text{ MVm}^{-1}$ ; 5:  $1.5 \text{ MVm}^{-1}$ ; 6:  $2.0 \text{ MVm}^{-1}$ ; 7:  $2.5 \text{ MVm}^{-1}$ .

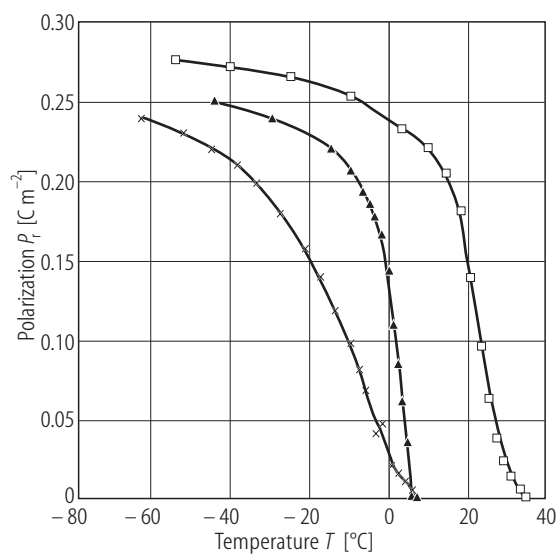


**Fig. 1B-c19-009.**  $\text{Pb}(\text{Sc}_{1/2}\text{Ta}_{1/2})\text{O}_3$  (ceramics).  $P_r$  vs.  $T$  [93Chu]. Open squares: stoichiometric highly ordered sample. Full triangles: stoichiometric highly disordered sample. Crosses: highly disordered sample with lead vacancies.

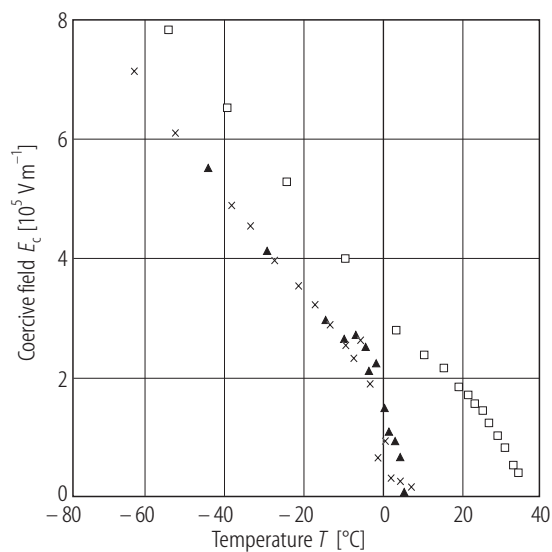


**Fig. 1B-c19-010.**  $\text{Pb}(\text{Sc}_{1/2}\text{Ta}_{1/2})\text{O}_3$  (ceramics).  $E_c$  vs.  $T$  [93Chu]. Open squares: stoichiometric highly ordered sample. Full triangles: stoichiometric highly disordered sample. Crosses: highly disordered sample with lead vacancies.

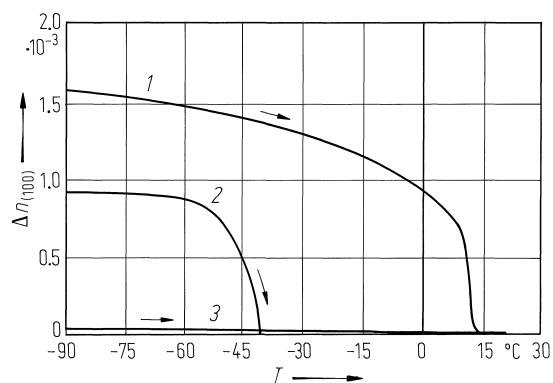


**Fig. 1B-c19-011.**  $\text{Pb}(\text{Sc}_{1/2}\text{Ta}_{1/2})\text{O}_3$  (ceramics).  $\Delta n_{(100)}$  vs.  $T$  [81Set]. Curve 1: ordered; 2: disordered, cooled under  $E$  of  $1 \cdot 10^3 \text{ kV m}^{-1}$ ; 3: disordered, cooled without  $E$ .  $\lambda = 632.8 \text{ nm}$ .

---

**References**

- 59Ism Ismailzade, I.G.: Kristallografiya **4** (1959) 417; Sov. Phys. Crystallogr. (English Transl.) **4** (1959) 389.
- 59Smo Smolenskii, G.A., Isupov, V.A., Agranovskaya, A.I.: Fiz. Tverd. Tela **1** (1959) 170; Sov. Phys. Solid State (English Transl.) **1** (1959) 150.
- 80Set1 Setter, N., Cross, L.E.: J. Cryst. Growth **50** (1980) 555.
- 80Set2 Setter, N., Cross, L.E.: Phys. Status Solidi (a) **61** (1980) K71.
- 81Set Setter, N., Cross, L.E.: Ferroelectrics **37** (1981) 551.
- 85Gro Groves, P.: J. Phys. C **18** (1985) L1073.
- 86Ran Randall, C.A., Barber, D.J., Whatmore, R.W., Groves, P.: J. Mater. Sci. **21** (1986) 4456.
- 91Pat Patel, A., Shorrocks, N.M., Whatmore, R.W.: IEEE Trans. Ultrason. Ferroelectr. Freq. Control **38** (1991) 672.
- 92Dag Daglish, M., Moulson, A.J.: Ferroelectrics **126** (1992) 215.
- 92Pen Peng, J., Bursill, L.A.: J. Computer-Assisted Microsc. **4** (1992) 309.
- 93Chu Chu, F., Setter, N., Tagantsev, A.K.: J. Appl. Phys. **74** (1993) 5129.
- 93Pen Peng, J., Bursill, L.A.: Mod. Phys. Lett. B **7** (1993) 609.